Radial Accommodation in the Ehrenfest Problem

A Conditional Layered-Ring Model with an Effective Covariant Phase-Stiffness Realization

S. M. H. Emamifar
Independent Research Collaboration on
Black Hole and Cosmology Concepts (IRCBHC)
ORCID: 0009-0007-6257-0163

Abstract

The Ehrenfest problem is traditionally formulated by considering an ideally Born-rigid disk accelerated from rest into uniform rotation. Tangential material elements are associated with local Lorentz contraction in an inertial laboratory frame, while radial elements are instantaneously perpendicular to the tangential motion and therefore do not undergo direct longitudinal Lorentz contraction. The further conclusion that the material radius must remain unchanged is, however, an additional mechanical assumption rather than a direct consequence of the Lorentz transformation.

A conditional layered-ring construction is presented. Each concentric material ring is allowed to change its laboratory radius while preserving the sum of its local comoving circumferential lengths. Under this closure condition, the stationary radial map is

$$r(\rho) = \frac{\rho}{\sqrt{1+\omega^2\rho^2/c^2}},$$

where ρ is the initial material radius and ω is the angular velocity of the final stationary configuration. The construction preserves

$$C_{\text{lab}} = 2\pi r$$

on laboratory simultaneity slices while satisfying

$$C_{\text{proper}} = \gamma C_{\text{lab}} = 2\pi\rho.$$

The kinematic construction is supplemented by an effective stationary radial-support model. Reducing a covariant spatial phase-gradient sector on a uniformly wound thin ring produces the proper circumference energy

$$U_{\text{wind}}(C) = \frac{\overline{K}_s}{2}\, C\left[\left(\frac{2\pi N}{C}\right)^2 - q_0^2\right]^2.$$

Its minimum fixes the summed local comoving circumference to

$$C_0 = \frac{2\pi|N|}{q_0},$$

and near that minimum the reduced theory yields

$$\kappa_{\text{eff}} = \frac{4\overline{K}_s q_0^4}{C_0}.$$

In the strong-locking limit, the stationary thin ring satisfies $C_{\text{proper}} = C_0$, and the radial map follows exactly. A phenomenological fixed-ω radial Lagrangian gives a finite-stiffness radius correction and a local radial stability condition within that reduced model.

The paper compares stationary nonrotating and uniformly rotating configurations. It does not model the transient spin-up process, a time-dependent torque law, or a Hamiltonian evolution between the two states. It also does not establish that all physical matter possesses the proposed phase sector or derive a complete continuous interacting disk. Finally, the geometric second moment of the mapped rest-mass distribution is derived; it must not be identified with the full relativistic dynamical moment of inertia.

As a separate observational extension, a dimensionless orbital-transfer template is applied to the published osculating orbit of the Galactic-centre star S2. For unit transfer amplitude, the first-stage simulation produces a maximum sky-plane residual of approximately 4.1 μas. This is not claimed as a direct consequence of the material-ring derivation, and no real S2 measurement table is fitted in the present work; it is presented as a falsifiable template for a future joint astrometric and spectroscopic fit.

1 Introduction

In 1909, Paul Ehrenfest examined the compatibility of rotational motion with Max Born's relativistic definition of rigidity. The problem showed that an extended body cannot, in general, be accelerated from rest into rotation while preserving all local proper distances throughout the spin-up process.

The classical argument is commonly summarized as follows:

1. The circumference of a rotating disk is tangential to the motion.
2. Tangential material elements are locally Lorentz-contracted when measured at one laboratory time.
3. The radius is instantaneously perpendicular to the tangential velocity.
4. It is then assumed that the material radius remains unchanged.
5. A contracted circumference and an unchanged radius appear to conflict with

$$C = 2\pi R.$$

The central observation of this paper is that the third statement does not logically imply the fourth.

From

no direct longitudinal Lorentz contraction along the radius,

one may conclude only that the standard longitudinal contraction formula does not act directly on a radial line element.

One may not automatically conclude that

the material radius cannot change dynamically.

A real radial displacement caused by forces, changing equilibrium separations, redistribution of matter, or a specified acceleration protocol is conceptually distinct from direct radial Lorentz contraction.

2 Scope of the Present Analysis

The present work compares two stationary endpoint configurations: an initially relaxed nonrotating disk and a final uniformly rotating layered configuration. It does not attempt to calculate the transient spin-up history connecting those endpoints.

Accordingly, the derivation does not require a time-dependent torque law, a law for the changing angular velocity, or a Hamiltonian description of the transition. Those questions concern the preparation and dynamical stability of the final state and are logically separate from the stationary circumference–radius consistency problem addressed here.

The central claim is conditional and stationary:

> If each material ring remains closed, preserves the sum of its local comoving circumferential lengths, and obeys the standard local Lorentz relation for tangential segments relative to the laboratory frame, then radial accommodation yields a self-consistent final radius.

The radius is not directly Lorentz-contracted. It changes through radial rearrangement of the material rings between the two stationary endpoint configurations.

3 What the Ehrenfest Argument Establishes

Born rigidity requires the orthogonal proper distance between neighboring worldlines of a material congruence to remain constant.

A disk initially at rest cannot be accelerated into rotation while preserving this condition everywhere. Different material radii acquire different tangential speeds,

$$v(r) = \omega r,$$

and consequently different acceleration histories and Lorentz factors.

The robust conclusion is therefore

$$\boxed{\text{A disk cannot be spun up from rest while remaining globally Born-rigid.}}$$

This does not imply

$$\boxed{\text{Every physical rotating disk must retain its original radius.}}$$

The first statement is a kinematic restriction. The second would be a dynamical prediction requiring a material law, forces, stresses, and boundary conditions.

4 Why Perfect Rigidity Is Not a Physical Property

No perfectly rigid macroscopic body is known to exist.

For a body to be perfectly rigid in the strongest classical sense, a displacement at one point would have to be communicated instantaneously to all other points:

$$v_{\text{mechanical}} \to \infty.$$

This is incompatible with relativistic causality.

Real disturbances propagate as elastic waves, stress waves, lattice excitations, or other collective modes with finite signal speed:

$$v_{\text{signal}} \leq c.$$

The argument does not require fundamental particles themselves to be extended, soft, or deformable. The constituents may be treated as pointlike. Macroscopic rigidity is a property of the relations among those constituents.

A perfectly rigid body would require

$$d_{ij} = \text{constant} \qquad \text{for every material pair } i, j.$$

Real interactions do not enforce this condition absolutely. Relative separations are maintained dynamically and may change under acceleration.

Near a stable equilibrium, a local interaction may be represented schematically as

$$F \simeq -k\,\Delta x.$$

The relevant physical statement is therefore:

> The constituents of an extended body are not geometrically fused into an immutable configuration. Their relative separations are maintained by finite-strength, finite-speed interactions and may change under stress or acceleration.

5 The Layered-Ring Representation

Consider an initially stationary disk of relaxed radius R_0.

Decompose the disk into a continuous family of concentric material rings. Let

$$0 \leq \rho \leq R_0$$

label the initial relaxed radius of a ring.

Its initial circumference is

$$C_0(\rho) = 2\pi\rho.$$

After uniform rotation is established, let the same material ring occupy laboratory radius

$$r = r(\rho).$$

Its tangential speed is

$$v(\rho) = \omega r(\rho),$$

and its Lorentz factor is

$$\gamma(\rho) = \frac{1}{\sqrt{1 - \omega^2 r(\rho)^2/c^2}}.$$

Every ring except the central point participates in relativistic motion. The disk therefore has a radial gradient of tangential speed and Lorentz factor.

6 Three Distinct Circumferential Quantities

A careful treatment must distinguish three quantities.

6.1 Initial relaxed circumference

$$C_0(\rho) = 2\pi\rho.$$

6.2 Laboratory circumference

At one laboratory time,

$$C_{\text{lab}}(\rho) = 2\pi r(\rho).$$

This relation refers to the Euclidean spatial geometry of an inertial laboratory simultaneity slice.

6.3 Sum of local comoving lengths

Each infinitesimal tangential element possesses an instantaneous local comoving inertial frame. Define

$$C_{\text{proper}}(\rho)$$

as the sum of those local proper lengths around the ring.

This is not the length of the full ring measured in one global inertial rest frame, because no such frame is comoving with the entire rotating circumference.

Locally,

$$\mathrm{d}\ell_{\text{lab}} = \frac{\mathrm{d}\ell_{\text{proper}}}{\gamma(\rho)}.$$

Since the tangential speed is constant around a ring of fixed radius, summing the local relation gives

$$C_{\text{proper}}(\rho) = \gamma(\rho) C_{\text{lab}}(\rho).$$

7 The Radial-Accommodation Condition

The proposed model imposes the conditional closure rule:

> Between the initial relaxed state and the final uniformly rotating state, each material ring is assumed to remain closed and to preserve the sum of its local comoving circumferential lengths, while being permitted to change its laboratory radius.

Thus,

$$C_{\text{proper,final}}(\rho) = C_{\text{proper,initial}}(\rho) = 2\pi\rho.$$

Using

$$C_{\text{proper,final}} = \gamma C_{\text{lab}}, \qquad C_{\text{lab}} = 2\pi r,$$

we obtain

$$2\pi\rho = \gamma(\rho)\, 2\pi r(\rho).$$

Therefore,

$$\boxed{r(\rho) = \frac{\rho}{\gamma(\rho)}.}$$

This does not represent direct radial Lorentz contraction. It is a radial rearrangement required by the imposed combination of ring closure, preserved summed local proper circumference, and tangential Lorentz contraction.

Changes in the equilibrium separations among material constituents may accommodate such a rearrangement, subject to the constitutive response and energy cost of the material.

8 Self-Consistent Radial Solution

Substituting

$$\gamma(\rho) = \frac{1}{\sqrt{1 - \omega^2 r(\rho)^2/c^2}}$$

into

$$r(\rho) = \frac{\rho}{\gamma(\rho)}$$

gives

$$r(\rho) = \rho\sqrt{1 - \frac{\omega^2 r(\rho)^2}{c^2}}.$$

Squaring,

$$r(\rho)^2 = \rho^2 - \frac{\omega^2\rho^2}{c^2} r(\rho)^2.$$

Hence,

$$r(\rho)^2 \left(1 + \frac{\omega^2\rho^2}{c^2}\right) = \rho^2.$$

The positive-radius solution is

$$\boxed{r(\rho) = \frac{\rho}{\sqrt{1 + \omega^2\rho^2/c^2}}.}$$

The final tangential speed is

$$v(\rho) = \frac{\omega\rho}{\sqrt{1 + \omega^2\rho^2/c^2}},$$

so

$$\frac{v(\rho)}{c} = \frac{\omega\rho/c}{\sqrt{1 + \omega^2\rho^2/c^2}} < 1.$$

The Lorentz factor becomes

$$\boxed{\gamma(\rho) = \sqrt{1 + \frac{\omega^2\rho^2}{c^2}}.}$$

For the outermost ring,

$$\rho = R_0,$$

the final radius is

$$\boxed{R = \frac{R_0}{\sqrt{1+\omega^2 R_0^2/c^2}} = \frac{R_0}{\gamma_e}.}$$

This result is conditional on the radial-accommodation closure rule.

9 Preservation of Ring Ordering

Differentiate

$$r(\rho) = \rho \left(1 + \frac{\omega^2 \rho^2}{c^2}\right)^{-1/2}.$$

Then

$$\boxed{\frac{\mathrm{d}r}{\mathrm{d}\rho} = \frac{1}{(1+\omega^2\rho^2/c^2)^{3/2}} = \frac{1}{\gamma(\rho)^3} > 0.}$$

Therefore,

$$\rho_1 < \rho_2 \quad \Longrightarrow \quad r(\rho_1) < r(\rho_2).$$

The rings do not cross.

However,

$$\frac{\mathrm{d}r}{\mathrm{d}\rho} < 1 \qquad (\rho > 0),$$

so the radial separation of neighboring rings decreases:

$$\mathrm{d}\rho \longrightarrow \mathrm{d}r = \frac{\mathrm{d}\rho}{\gamma(\rho)^3}.$$

This is an anisotropic deformation rather than direct radial Lorentz contraction.

10 Circumference and Euclidean Closure

The laboratory circumference is

$$C_{\text{lab}}(\rho) = 2\pi r(\rho) = \frac{2\pi\rho}{\sqrt{1+\omega^2\rho^2/c^2}}.$$

Since

$$\gamma(\rho) = \sqrt{1+\omega^2\rho^2/c^2},$$

we have

$$\boxed{C_{\text{lab}}(\rho) = \frac{C_0(\rho)}{\gamma(\rho)}.}$$

At the same time,

$$\boxed{C_{\text{lab}}(\rho) = 2\pi r(\rho).}$$

The summed local comoving circumference is

$$C_{\text{proper}}(\rho) = \gamma(\rho) C_{\text{lab}}(\rho) = 2\pi\rho.$$

Thus,

$$\boxed{C_{\text{proper,final}}(\rho) = C_{\text{proper,initial}}(\rho).}$$

In the final accommodated configuration, the laboratory circle has the reduced radius at which the locally Lorentz-contracted laboratory lengths close without a gap.

11 Removal of the Apparent Contradiction

The simplified paradox attempts to impose

$$R = R_0, \qquad C_{\text{lab}} = \frac{C_0}{\gamma_e}, \qquad C_{\text{lab}} = 2\pi R.$$

Together these imply

$$2\pi R_0 = \frac{2\pi R_0}{\gamma_e},$$

which is impossible for

$$\gamma_e > 1.$$

The radial-accommodation model rejects the fixed-radius condition:

$$R \neq R_0.$$

Instead,

$$R = \frac{R_0}{\gamma_e}.$$

Consequently,

$$C_{\text{lab}} = 2\pi R = 2\pi \frac{R_0}{\gamma_e} = \frac{C_0}{\gamma_e}.$$

Therefore,

$$\boxed{C_{\text{lab}} = 2\pi R,}$$

$$\boxed{C_{\text{lab}} = \frac{C_0}{\gamma_e},}$$

and

$$\boxed{C_{\text{proper}} = C_0}$$

can hold simultaneously.

12 Comparison with a Fixed-Radius Constraint

Suppose a ring of initial proper circumference C_0 preserves its local proper lengths while an external constraint forces its path radius to remain unchanged.

Its total laboratory material length would be

$$C_{\text{material,lab}} = \frac{C_0}{\gamma}.$$

The fixed circular path would retain circumference

$$C_{\text{path}} = C_0.$$

The resulting mismatch would be

$$\Delta C = C_0 \left(1 - \frac{1}{\gamma}\right).$$

Depending on the acceleration protocol and material law, the ring may develop a gap, stretch, sustain internal stress, or fail.

Radial accommodation instead imposes

$$2\pi r = \frac{C_0}{\gamma},$$

so

$$\Delta C = 0.$$

This is one consistent boundary condition, not the only possible physical response.

13 Born Rigidity and Anisotropic Deformation

The construction does not assume that the transition to the final state is Born-rigid. The transient spin-up process itself is outside the scope of the present analysis.

Tangentially,

$$\frac{C_{\text{proper,final}}}{C_{\text{proper,initial}}} = 1.$$

Radially,

$$\frac{\mathrm{d}r}{\mathrm{d}\rho} = \frac{1}{\gamma(\rho)^3} < 1.$$

The final state may therefore involve:

- reduced radial spacing;
- changing surface density;
- radial compression;
- shear between neighboring layers;
- nonuniform stress;
- redistribution of stored elastic or field energy.

The violation of perfect rigidity is not itself a physical defect, because perfect rigidity is not physically available.

The relevant question is:

> Which non-rigid deformation follows from a specified material law, stress–energy tensor, and acceleration protocol?

14 From Kinematics to Stationary Radial Support

Lorentz contraction is not a force.

The radial map

$$r(\rho) = \frac{\rho}{\sqrt{1 + \omega^2\rho^2/c^2}}$$

was first obtained from three conditional kinematic requirements:

1. each material ring remains closed;
2. its summed local comoving circumference is preserved;
3. its laboratory tangential lengths satisfy the local Lorentz relation.

At the purely geometrical level, these conditions define a self-consistent endpoint but do not specify which interaction supplies the required radial force.

Section 16 introduces a covariant phase-gradient sector. Appendix A reduces that sector to a uniformly wound thin ring and obtains an explicit circumference-dependent energy. In the strong-locking limit, the reduced action enforces

$$C_{\text{proper}} = C_0$$

and produces the radial-accommodation map. At finite stiffness, it gives a small radius correction and a reduced-model stability condition.

The resulting classification is therefore

$$\boxed{\text{a conditional radial map with an explicit effective fixed-}\omega\text{ radial support mechanism for a thin ring}}$$

The remaining problem is not the mathematical absence of any possible radial force. It is to determine whether physical matter possesses the proposed phase sector, to derive its parameters from a microscopic model, and to extend the thin-ring reduction to a continuous interacting disk with a complete stress–energy tensor.

15 Externally Supported Radial Accommodation

An external mechanical or gravitational field can contribute to the radial force balance, but a clock-rate gradient is not by itself a force.

For a weak, stationary gravitational field with potential Φ, the metric may be written approximately as

$$\mathrm{d}s^2 \simeq -\left(1+\frac{2\Phi}{c^2}\right)c^2\mathrm{d}t^2 + \left(1-\frac{2\Phi}{c^2}\right)\mathrm{d}\boldsymbol{x}^2.$$

For a slowly moving material element,

$$\frac{\mathrm{d}\tau}{\mathrm{d}t} \simeq 1 + \frac{\Phi}{c^2} - \frac{v^2}{2c^2}.$$

Equivalently,

$$\Gamma_{\text{tot}} \equiv \frac{\mathrm{d}t}{\mathrm{d}\tau} \simeq 1 - \frac{\Phi}{c^2} + \frac{v^2}{2c^2}.$$

The potential contributes a real radial force through its spatial gradient. In a nonrelativistic axisymmetric approximation, radial equilibrium may be written schematically as

$$\frac{\mathrm{d}\sigma_r}{\mathrm{d}r} + \frac{\sigma_r - \sigma_\phi}{r} + \mu\left(\omega^2 r - \frac{\mathrm{d}\Phi}{\mathrm{d}r}\right) = 0,$$

where σ_r and σ_ϕ are radial and hoop stresses and μ is the mass density.

This equation does not, by itself, imply the radial-accommodation map. The map must be obtained by solving the equilibrium equations together with a constitutive relation and boundary conditions.

An externally chosen potential may be designed to support the target profile. Such a result would establish existence under engineered forcing, not a universal spontaneous mechanism.

The effective centrifugal potential

$$\Phi_{\mathrm{cf}} = -\frac{1}{2}\omega^2 r^2$$

is a rotating-frame inertial potential. It must not automatically be identified with a gravitational field generated by the rotating matter.

16 A Candidate Covariant Phase-Locking Extension

This section introduces an effective microscopic extension. The covariant field sector is a model hypothesis. Its thin-ring reduction and its relation to the radial map are derived explicitly in Appendix A.

16.1 Phase-capacity variables

To avoid confusion with the disk radius, denote the internal channel, progression channel, and total phase capacity by

$$\mathcal{R}, \qquad \mathcal{K}, \qquad \mathcal{Q}_0.$$

The proposed closure relation is

$$\boxed{\mathcal{R}^2 + \mathcal{K}^2 = \mathcal{Q}_0^2.}$$

This constraint alone does not imply

$$\mathcal{R} = \mathcal{K}.$$

An equal-channel equilibrium may be represented by the energy density

$$U_{\mathrm{eq}} = \frac{\lambda_{\mathrm{eq}}}{2}\left(\mathcal{R} - \mathcal{K}\right)^2 + \frac{\Lambda_{\mathrm{eq}}}{2}\left(\mathcal{R}^2 + \mathcal{K}^2 - \mathcal{Q}_0^2\right)^2,$$

where

$$\lambda_{\mathrm{eq}} > 0, \qquad \Lambda_{\mathrm{eq}} > 0.$$

Its minimum satisfies

$$\mathcal{R} = \mathcal{K}, \qquad \mathcal{R}^2 + \mathcal{K}^2 = \mathcal{Q}_0^2,$$

and therefore

$$\mathcal{R} = \mathcal{K} = \frac{\mathcal{Q}_0}{\sqrt{2}}.$$

This is an explicit model assumption generated by an energy function, rather than a consequence of the quadratic closure relation alone.

16.2 Phase winding and proper circumference

Let a complex material phase field be

$$\Psi = Ae^{i\phi}.$$

On a closed spatial material loop Σ, define the phase winding number

$$N = \frac{1}{2\pi} \oint_{\Sigma} \mathrm{d}\phi \in \mathbb{Z}.$$

This is a spatial loop integral. It must not be confused with an integral of proper time along a timelike worldline.

For a uniform winding on a loop with summed local comoving circumference C_{proper}, the proper wavenumber is

$$q = \frac{2\pi N}{C_{\text{proper}}}.$$

Conservation of N alone does not conserve C_{proper}, because the wavenumber q may change. A sufficient additional dynamical condition is the selection of a preferred nonzero proper wavenumber q_0.

The spatial phase-gradient sector introduced below penalizes departures of q^2 from q_0^2. For a fixed winding sector, its lowest-energy circumference is therefore

$$\boxed{C_0 = \frac{2\pi|N|}{q_0}.}$$

Thus, circumference locking follows conditionally from two ingredients: topological conservation of N and dynamical selection of q_0.

16.3 Covariant spatial phase-field sector

For the stationary claims made in this paper, only the spatial phase-gradient sector is required. Consider

$$S = \int \sqrt{-g}\, \mathcal{L}\, \mathrm{d}^4 x,$$

with

$$\mathcal{L} = -\varepsilon(n, s_{AB}) - \frac{K_s}{2} \left(h^{\mu\nu} \nabla_\mu \phi \nabla_\nu \phi - q_0^2\right)^2 - U_{\text{eq}}.$$

Here:

- u^μ is the material four-velocity, normalized by $u^\mu u_\mu = -c^2$;
- n is the material number density;
- s_{AB} denotes material strain variables;
- $\varepsilon(n, s_{AB})$ is the non-phase material energy density;
- ϕ is the phase field;
- $q_0 > 0$ is the preferred proper spatial wavenumber;
- $K_s > 0$ is the spatial phase-gradient stiffness;

- $$h^{\mu\nu} = g^{\mu\nu} + \frac{u^\mu u^\nu}{c^2}$$
  is the projector into the instantaneous local rest space.

The displayed terms are constructed from Lorentz-covariant scalars. In this paper the sector is reduced only on stationary, uniformly wound ring configurations. No law for transient phase evolution is asserted or required for the stationary endpoint argument.

For a stationary, uniformly wound thin ring, the spatial phase-gradient term can be reduced explicitly. Appendix A shows that the reduction produces

$$U_{\text{wind}}(C) = \frac{\overline{K}_s}{2}\, C \left[\left(\frac{2\pi N}{C}\right)^2 - q_0^2\right]^2 .$$

The minimum is at

$$C = C_0 = \frac{2\pi|N|}{q_0},$$

and the near-minimum form is

$$U_{\text{wind}} = \frac{\kappa_{\text{eff}}}{2}(C - C_0)^2 + \mathcal{O}\Big((C - C_0)^3\Big)\,,$$

with

$$\boxed{\kappa_{\text{eff}} = \frac{4\overline{K}_s q_0^4}{C_0}.}$$

In the strong-locking limit, variation of the reduced ring action enforces

$$C_{\text{proper}} = C_0$$

and yields the radial map

$$r(\rho) = \frac{\rho}{\sqrt{1 + \omega^2\rho^2/c^2}}.$$

This establishes the stationary thin-ring equilibrium at the effective level. Extending the result to a continuous interacting disk and deriving the coefficients from a deeper microscopic theory remain separate tasks. The transient preparation of the rotating state is not part of the present derivation.

16.4 Reference metric and low-stress accommodation

A changing geometric radius generally produces strain relative to the initial stress-free state.

For radial accommodation to occur with small residual material stress, the phase sector would have to modify the preferred material metric:

$$G^{(0)}_{AB} \longrightarrow G^{(\text{phase})}_{AB}(\omega).$$

The thin-ring reduction proves the existence of an effective circumference-locking force. It does not by itself derive the full two-dimensional reference metric of a disk or prove that radial and shear stresses remain small. Those questions require a constitutive extension of the field model and the associated stress–energy tensor.

17 Corrected Geometric Second Moment

Consider a thin disk with uniform initial rest surface density σ_0.

The initial rest mass is

$$M = \pi\sigma_0 R_0^2,$$

and its initial geometric second moment is

$$I_0 = \frac{1}{2}MR_0^2 = \frac{1}{2}\pi\sigma_0 R_0^4.$$

Under the radial map

$$r(\rho) = \frac{\rho}{\sqrt{1+\omega^2\rho^2/c^2}},$$

define the mapped rest-mass second moment

$$I_{\rm geom}(\omega) = \int r^2\,\mathrm{d}m_0.$$

Since

$$\mathrm{d}m_0 = 2\pi\sigma_0\rho\,\mathrm{d}\rho,$$

we obtain

$$I_{\rm geom}(\omega) = 2\pi\sigma_0\int_0^{R_0}\frac{\rho^3}{1+\omega^2\rho^2/c^2}\,\mathrm{d}\rho.$$

Introduce

$$x = \frac{\omega^2 R_0^2}{c^2}.$$

The integral gives

$$I_{\rm geom}(\omega) = \pi\sigma_0\left[\frac{R_0^2c^2}{\omega^2} - \frac{c^4}{\omega^4}\ln(1+x)\right].$$

Therefore,

$$\boxed{\frac{I_{\rm geom}(\omega)}{I_0} = \frac{2}{x^2}\left[x-\ln(1+x)\right].}$$

For

$$x \ll 1,$$

the expansion is

$$\boxed{\frac{I_{\rm geom}(\omega)}{I_0} = 1 - \frac{2}{3}x + \frac{1}{2}x^2 - \frac{2}{5}x^3 + \mathcal{O}(x^4).}$$

Thus, under the assumed map,

$$I_{\rm geom}(\omega) < I_0$$

for positive ω.

However,

$$I_{\rm geom} = \int r^2\,\mathrm{d}m_0$$

is only a geometric second moment of the rest-mass distribution.

The full relativistic angular momentum must be derived from the stress–energy tensor:

$$J = \int T^0{}_\phi \sqrt{-g}\, \mathrm{d}^3x.$$

Possible dynamical definitions include

$$I_{\text{eff}} = \frac{J}{\omega}$$

and

$$I_{\text{response}} = \frac{\mathrm{d}J}{\mathrm{d}\omega}.$$

These quantities may contain contributions from kinetic energy, elastic energy, phase-field energy, and internal stresses. Consequently, I_{geom} must not yet be advertised as the complete relativistic moment of inertia.

18 What the Model Establishes

The radial-accommodation construction establishes the conditional kinematic result:

> If each concentric material ring remains closed, preserves its summed local comoving circumference, and is free to change its laboratory radius, then there exists a monotonic self-consistent radial map for which the local tangential Lorentz relation and Euclidean laboratory closure hold simultaneously.

The map is

$$\boxed{r(\rho) = \frac{\rho}{\sqrt{1 + \omega^2\rho^2/c^2}}.}$$

The construction demonstrates that

$$\boxed{\text{absence of direct radial Lorentz contraction}}$$

does not imply

$$\boxed{\text{absence of dynamical radial deformation.}}$$

It also shows that the circumference–radius contradiction depends on maintaining the additional fixed-radius condition.

In addition, Appendix A shows that the proposed covariant spatial phase-gradient sector reduces, for a uniformly wound thin ring, to a definite circumference energy. In the strong-locking limit, the reduced action supports the exact radial map. At finite stiffness, it gives

$$\boxed{\delta r \simeq \frac{M_0\omega^2 r_0}{4\pi^2 \kappa_{\text{eff}} \gamma_0^5}.}$$

Within the reduced fixed-ω model, the strong-locking branch is locally stable when

$$\boxed{\kappa_{\text{eff}} > \frac{M_0\omega^2}{4\pi^2\gamma_0^3}.}$$

The model therefore establishes both a kinematically consistent stationary endpoint and an effective constrained fixed-ω radial-equilibrium realization for a thin ring.

19 What the Model Does Not Yet Establish

The present derivation does not prove that every physical rotating disk must contract according to the proposed map.

A real disk may:

- expand because of centrifugal stress;
- contract under external radial forcing;
- stretch circumferentially;
- develop nonuniform density;
- shear;
- form a gap;
- oscillate;
- tear or fail.

The model does not invalidate the Herglotz–Noether theorem. It does not claim that the final configuration is produced by a globally Born-rigid spin-up process; the transient preparation is outside the scope of the paper.

It also does not eliminate the synchronization and clock-comparison issues associated with rotating observers.

The gravitational discussion establishes only that an external field may participate in radial force balance.

For a uniformly wound thin ring, the phase-gradient action has been shown to produce the radial map in the strong-locking limit and a locally stable finite-stiffness branch under the condition derived in Appendix A. The remaining limitations are:

- extension from one thin ring to a continuous interacting disk;
- derivation of the phase coefficients from a microscopic theory of matter;
- construction of the complete stress–energy tensor;
- determination of the two-dimensional material reference metric;
- comparison with ordinary relativistic elasticity;
- independent determination of the parameters entering the finite-stiffness correction;
- direct derivation of the finite-stiffness correction from the unreduced covariant action.

20 Relation to General Relativity

The rotating-disk problem played a role in the historical development of ideas concerning accelerated frames and operational geometry.

However, general relativity was not derived solely from the Ehrenfest problem. It also arose from the equivalence principle, gravitational clock effects, the Newtonian limit, the motion of light, the anomalous perihelion advance of Mercury, and the search for generally covariant field equations.

A successful radial-accommodation model would therefore establish only that one material response to rotation can preserve Euclidean laboratory closure without imposing a fixed radius.

It would not, by itself, refute general relativity.

The defensible conclusion is

The Ehrenfest disk is not an independent proof that physical spacetime must be curved.

21 Research Program

The thin-ring reduction supplies an effective constrained fixed-ω radial-equilibrium realization. Turning this stationary result into a predictive theory of a continuous disk requires the following further steps.

21.1 Continuous constitutive model

Specify

$$\varepsilon = \varepsilon\left(n, s_{AB}, \phi, \nabla\phi, \ldots\right)$$

for interacting radial layers, including radial, hoop, and shear responses.

21.2 Stress–energy tensor

Derive

$$T^{\mu\nu} = -\frac{2}{\sqrt{-g}}\frac{\delta S}{\delta g_{\mu\nu}}$$

including material, elastic, and phase-gradient contributions.

21.3 Continuous equations of motion

Solve

$$\nabla_\mu T^{\mu\nu} = f^{\nu}_{\text{external}},$$

or

$$\nabla_\mu T^{\mu\nu} = 0$$

for an isolated model, together with the phase-field and material-map equations.

21.4 Disk equilibrium

Determine whether the family of ring solutions can coexist as a continuous disk without inconsistent inter-ring shear or radial stress, and whether

$$r_{\mathrm{eq}}(\rho) = \frac{\rho}{\sqrt{1+\omega^2\rho^2/c^2}}$$

remains the equilibrium profile after all couplings are included.

21.5 Global stability

Study perturbations of the coupled disk,

$$r(\rho,\tau) = r_{\mathrm{eq}}(\rho) + \delta r(\rho,\tau),$$

including radial, azimuthal, and shear modes.

21.6 Phenomenological orbital transfer test

As a separate observational program, fit the dimensionless transfer coefficient η defined in Appendix C to the S2 astrometric and spectroscopic data. The fit must be performed jointly with the central mass, Galactic-centre distance, orbital elements, reference-frame offsets and drifts, light-travel-time corrections, redshift terms, and relativistic precession. A credible detection would require a common value of η to improve both astrometric and spectroscopic residuals and, where the data permit, to remain consistent across several short-period stars.

21.7 Observable quantities

Calculate

$$J(\omega), \qquad E(\omega), \qquad I_{\mathrm{eff}}(\omega),$$

from the full stress–energy tensor, and compare them with standard relativistic elastic-disk models.

22 Conclusion

The Ehrenfest problem retains mathematical importance as a demonstration that arbitrary spin-up is incompatible with perfect Born rigidity.

Its direct relevance to real material disks is more limited because real extended bodies are not perfectly rigid. Their constituents remain distinct, and their relative separations are maintained dynamically.

The inference

$$\text{radial direction is perpendicular to tangential motion}$$
$$\Downarrow$$
$$\text{radius must remain unchanged}$$

is not logically compulsory.

The valid conclusion is only that direct longitudinal Lorentz contraction does not act along the radial direction.

Under the conditional preservation of each ring's summed local comoving circumference, the radial map is

$$\boxed{r(\rho) = \frac{\rho}{\sqrt{1+\omega^2\rho^2/c^2}}.}$$

For the outer edge,

$$\boxed{R = \frac{R_0}{\sqrt{1+\omega^2 R_0^2/c^2}} = \frac{R_0}{\gamma_e}.}$$

This configuration satisfies

$$C_{\mathrm{lab}} = 2\pi R = \frac{C_0}{\gamma_e}$$

while preserving

$$C_{\mathrm{proper}} = C_0.$$

The construction is mathematically closed at the stationary kinematic level and admits an explicit effective constrained fixed-ω radial-equilibrium realization for a uniformly wound thin ring.

Reduction of the proposed covariant phase-gradient sector gives

$$U_{\mathrm{wind}}(C) = \frac{\overline{K}_s}{2}\, C \left[\left(\frac{2\pi N}{C}\right)^2 - q_0^2\right]^2 .$$

The preferred summed local comoving circumference is

$$C_0 = \frac{2\pi|N|}{q_0},$$

and the corresponding near-equilibrium stiffness is

$$\kappa_{\mathrm{eff}} = \frac{4\overline{K}_s q_0^4}{C_0}.$$

In the strong-locking limit, the radial map follows exactly. At finite stiffness, the reduced model gives

$$\delta r \simeq \frac{M_0\omega^2 r_0}{4\pi^2\kappa_{\mathrm{eff}}\gamma_0^5},$$

and the fixed-ω equilibrium is locally stable when

$$\kappa_{\mathrm{eff}} > \frac{M_0\omega^2}{4\pi^2\gamma_0^3}.$$

The model therefore advances beyond a force-free stationary kinematic construction: it possesses a concrete effective radial support mechanism within the reduced fixed-ω thin-ring model.

The appropriate final conclusion is

$$\boxed{\text{The Ehrenfest problem constrains Born-rigid rotation,}}$$

but

$$\boxed{\text{it does not uniquely determine the deformation of real rotating matter.}}$$

Appendix C also formulates a separate observational null test by transferring the radial factor to an orbital tracer through a free coefficient η. This extension is explicitly phenomenological: it is not used to derive or validate the stationary material-ring result.

The remaining work is to determine whether the effective phase sector is realized in physical matter, to derive its parameters microscopically, and to extend the thin-ring result to a complete continuous-disk theory. The transient spin-up history is a separate future problem and is not needed for the stationary consistency result established here.

A Effective Spatial Phase-Stiffness and Stationary Radial Support

This appendix closes the effective mathematical gap between the covariant phase-field action introduced in Section 16 and the circumference-locking energy required to support the radial-accommodation map.

The derivation does not claim that the proposed phase sector is already established as a fundamental description of physical matter. It shows, however, that the effective circumference stiffness need not be inserted as an unrelated potential. It follows from the spatial phase-gradient sector of the covariant action after reduction to a stationary, uniformly wound thin ring.

A.1 Reduction of the covariant phase sector

Consider the spatial phase-gradient contribution

$$\mathcal{L}_s = -\frac{K_s}{2}\left(h^{\mu\nu}\nabla_\mu\phi\nabla_\nu\phi - q_0^2\right)^2.$$

For a thin ring, integrate the phase energy over its proper transverse cross-section and any stationary amplitude profile. Denote the resulting effective one-dimensional coupling by

$$\overline{K}_s > 0.$$

Let

$$C \equiv C_{\text{proper}}$$

be the summed local comoving circumference.

For a stationary uniform phase winding,

$$N = \frac{1}{2\pi}\oint_\Sigma \mathrm{d}\phi \in \mathbb{Z}.$$

For definiteness take $N \neq 0$. The magnitude of the uniform proper wavenumber is

$$q = \frac{2\pi|N|}{C}.$$

The reduced phase-gradient energy is therefore

$$U_{\text{wind}}(C) = \frac{\overline{K}_s}{2}\,C\left[\left(\frac{2\pi N}{C}\right)^2 - q_0^2\right]^2. \tag{1}$$

This expression is nonnegative and vanishes when

$$q = q_0.$$

Its preferred circumference is consequently

$$\boxed{C_0 = \frac{2\pi|N|}{q_0}.} \tag{2}$$

Thus, conservation of the winding number alone does not fix the circumference. Conservation of N, together with dynamical selection of q_0, selects C_0.

A.2 Derived effective circumference stiffness

Write

$$C = C_0 + \Delta C, \qquad |\Delta C| \ll C_0.$$

Using

$$2\pi|N| = q_0 C_0,$$

equation (1) becomes

$$U_{\text{wind}}(C) = \frac{\overline{K}_s q_0^4}{2}\, C \left[\left(\frac{C_0}{C}\right)^2 - 1\right]^2.$$

Expanding about $C = C_0$ gives

$$U_{\text{wind}}(C) = \frac{2\overline{K}_s q_0^4}{C_0}(\Delta C)^2 + \mathcal{O}\Big((\Delta C)^3\Big).$$

Therefore,

$$U_{\text{wind}}(C) = \frac{\kappa_{\text{eff}}}{2}(C - C_0)^2 + \mathcal{O}\Big((C - C_0)^3\Big), \tag{3}$$

where

$$\boxed{\kappa_{\text{eff}} = \frac{4\overline{K}_s q_0^4}{C_0}.} \tag{4}$$

The effective circumference stiffness is thus related to the reduced phase-gradient coupling, the preferred proper wavenumber, and the winding circumference.

A.3 Effective radial Lagrangian

Consider a thin ring with non-phase rest mass M_0, initial relaxed radius ρ, laboratory radius $r(t)$, and externally prescribed constant angular velocity ω. The reference phase energy vanishes at $C = C_0$, so M_0 does not double-count the excess phase-gradient energy.

The mechanical Lagrangian is

$$L_{\text{mech}} = -M_0 c^2 \sqrt{1 - \frac{\dot{r}^2 + \omega^2 r^2}{c^2}}. \tag{5}$$

For stationary configurations define

$$\gamma_\omega(r) = \frac{1}{\sqrt{1 - \omega^2 r^2 / c^2}}.$$

The summed local comoving circumference is

$$C(r) = 2\pi r \gamma_\omega(r). \tag{6}$$

For adiabatic radial variations, consider the following phenomenological fixed-ω radial Lagrangian built from the proper circumference energy:

$$L_{\text{ring}} = -M_0 c^2 \sqrt{1 - \frac{\dot{r}^{\,2} + \omega^2 r^2}{c^2}} - U_{\text{wind}}(C(r))\,. \tag{7}$$

The circumference relation in (6) is evaluated with the instantaneous tangential Lorentz factor. The subsequent stability analysis is therefore a phenomenological quasi-static radial analysis at fixed ω, rather than a complete reduction of the covariant field theory. This distinction does not change the strong-locking minimum, but the finite-stiffness correction should ultimately be rederived from the unreduced covariant action.

For the ring initially labelled by ρ,

$$C_0 = 2\pi\rho.$$

A.4 Strong-locking limit and the exact radial map

In the strong-locking limit,

$$\overline{K}_s \to \infty,$$

any finite departure from $q = q_0$ has divergent energy. The stationary condition is therefore

$$C(r) = C_0.$$

Using

$$C(r) = 2\pi r \gamma_\omega(r), \qquad C_0 = 2\pi\rho,$$

we obtain

$$r\gamma_\omega(r) = \rho. \tag{8}$$

Solving for the positive radius gives

$$\boxed{r_0(\rho) = \frac{\rho}{\sqrt{1 + \omega^2\rho^2/c^2}}.} \tag{9}$$

The corresponding Lorentz factor is

$$\gamma_0(\rho) = \sqrt{1 + \frac{\omega^2\rho^2}{c^2}}.$$

Thus, within the strong phase-locking limit, the radial-accommodation map follows from the reduced phase-gradient energy.

A.5 Equivalent exact constraint formulation

The strong-locking limit may equivalently be represented by a Lagrange multiplier $\mathcal{T}$ with dimensions of force:

$$L_{\text{constr}} = -M_0 c^2 \sqrt{1 - \frac{\dot{r}^{\,2} + \omega^2 r^2}{c^2}} - \mathcal{T}\left[C(r) - C_0\right]. \tag{10}$$

Variation with respect to $\mathcal{T}$ gives

$$C(r) = C_0,$$

and hence the radial map (9).

For a stationary configuration,

$$\dot{r} = 0, \qquad \frac{\mathrm{d}C}{\mathrm{d}r} = 2\pi\gamma_\omega^3.$$

Variation with respect to r gives

$$M_0\gamma_\omega\omega^2 r - 2\pi\mathcal{T}\gamma_\omega^3 = 0.$$

Therefore,

$$\boxed{\mathcal{T} = \frac{M_0\omega^2 r}{2\pi\gamma_\omega^2}.} \tag{11}$$

The corresponding inward generalized radial force is

$$F_{\text{phase}} = \mathcal{T}\frac{\mathrm{d}C}{\mathrm{d}r}.$$

Hence,

$$\boxed{F_{\text{phase}} = M_0\gamma_\omega\omega^2 r.} \tag{12}$$

This balances the outward relativistic circular-motion term in the stationary reduced equation.

A.6 Finite-stiffness equilibrium

For finite phase stiffness use the quadratic approximation

$$U_{\text{wind}} \simeq \frac{\kappa_{\text{eff}}}{2}\left[C(r) - C_0\right]^2.$$

At $\dot{r} = 0$, the radial equilibrium equation is

$$M_0\gamma_\omega\omega^2 r - \kappa_{\text{eff}}\left[C(r) - C_0\right]\frac{\mathrm{d}C}{\mathrm{d}r} = 0. \tag{13}$$

Using

$$C(r) = 2\pi r\gamma_\omega, \qquad \frac{\mathrm{d}C}{\mathrm{d}r} = 2\pi\gamma_\omega^3,$$

this becomes

$$M_0\gamma_\omega\omega^2 r - 4\pi^2\kappa_{\text{eff}}\left(r\gamma_\omega - \rho\right)\gamma_\omega^3 = 0.$$

Let

$$r = r_0 + \delta r, \qquad |\delta r| \ll r_0,$$

where r_0 is the strong-locking solution. Since

$$r_0\gamma_0 = \rho$$

and

$$\frac{\mathrm{d}}{\mathrm{d}r}(r\gamma_\omega)\bigg|_{r_0} = \gamma_0^3,$$

the leading correction is

$$\boxed{\delta r \simeq \frac{M_0\omega^2 r_0}{4\pi^2\kappa_{\mathrm{eff}}\gamma_0^5}.} \tag{14}$$

The correction is positive. Finite phase stiffness therefore permits a small centrifugal expansion relative to the strong-locking radius.

Using equation (4), the correction may also be written as

$$\boxed{\delta r \simeq \frac{M_0\omega^2 r_0 C_0}{16\pi^2\overline{K}_s q_0^4\gamma_0^5}.} \tag{15}$$

A.7 Reduced-model local radial stability

Existence of a stationary solution does not by itself imply stability.

For small radial speeds, expand the mechanical Lagrangian about the stationary state:

$$L_{\mathrm{mech}} = -\frac{M_0c^2}{\gamma_\omega} + \frac{1}{2}M_0\gamma_\omega\dot{r}^2 + \mathcal{O}(\dot{r}^4).$$

The effective radial inertial coefficient at r_0 is

$$M_{\mathrm{rad,eff}} = M_0\gamma_0.$$

At the strong-locking point, the curvature of the quadratic phase energy is

$$U''_{\mathrm{wind}}(r_0) = \kappa_{\mathrm{eff}}\left(\frac{\mathrm{d}C}{\mathrm{d}r}\right)^2_{r_0} = 4\pi^2\kappa_{\mathrm{eff}}\gamma_0^6.$$

The radial derivative of the outward mechanical term is

$$\frac{\mathrm{d}}{\mathrm{d}r}\left(M_0\gamma_\omega\omega^2 r\right)\bigg|_{r_0} = M_0\omega^2\gamma_0^3.$$

Within the reduced fixed-ω model, local stability requires

$$4\pi^2\kappa_{\mathrm{eff}}\gamma_0^6 - M_0\omega^2\gamma_0^3 > 0.$$

Thus,

$$\boxed{\kappa_{\mathrm{eff}} > \frac{M_0\omega^2}{4\pi^2\gamma_0^3}.} \tag{16}$$

Using equation (4), this becomes

$$\boxed{\overline{K}_s > \frac{M_0\omega^2 C_0}{16\pi^2 q_0^4 \gamma_0^3}.} \tag{17}$$

The approximate squared frequency of small radial oscillations is

$$\boxed{\Omega_r^2 \simeq \frac{4\pi^2 \kappa_{\text{eff}}\gamma_0^5}{M_0} - \omega^2\gamma_0^2.} \tag{18}$$

A positive value of Ω_r^2 is equivalent to the reduced-model stability condition.

A.8 Kinematic phase-tilt parameter

The internal phase-tilt angle may be parametrized by

$$\boxed{\sin\theta = \frac{v}{c}.}$$

Then

$$\cos\theta = \sqrt{1 - \frac{v^2}{c^2}} = \frac{1}{\gamma},$$

and

$$\frac{1}{\cos\theta} = \gamma.$$

This is an internal kinematic parametrization of the phase-capacity decomposition. It is not the special-relativistic addition law for two ordinary spacetime velocities.

The quantitative circumference relation remains

$$C_{\text{proper}} = \gamma C_{\text{lab}}.$$

A.9 Scope of the effective derivation

The appendix establishes the following conditional result:

> If matter possesses the proposed covariant spatial phase-gradient sector, and if a thin ring carries a conserved uniform phase winding, then the reduced sector produces a definite circumference energy. In the strong-locking limit, the radial-accommodation map is the exact stationary constraint. At finite stiffness, the reduced model predicts a positive radius correction and a local fixed-ω stability condition.

The derivation therefore establishes

$$\boxed{\text{an effective constrained fixed-}\omega\text{ radial realization of the map for a thin ring.}}$$

It does not by itself establish that all physical matter possesses this phase sector, nor does it derive the numerical values of $\overline{K}_s$ and q_0 from a more fundamental microscopic theory. The finite-stiffness correction and stability condition belong to the phenomenological fixed-ω radial Lagrangian used above; they have not yet been derived directly from the unreduced covariant action. The appendix also does not replace the full continuous-disk stress–energy calculation.

B Scope of the Stationary Endpoint Analysis

The present paper compares an initial relaxed configuration with a final uniformly rotating stationary configuration. It does not calculate how the angular velocity changes with time or which torque history prepares the final state.

The stationary radial map follows from three assumptions: each material ring remains closed, the sum of its local comoving circumferential lengths is preserved, and its tangential segments satisfy the standard local Lorentz relation relative to the laboratory frame. These assumptions give

$$r(\rho) = \frac{\rho}{\sqrt{1 + \omega^2\rho^2/c^2}}.$$

The fixed-ω phase-stiffness model of Appendix A supplies an effective stationary radial support mechanism for a thin ring. Neither the radial map nor the stationary force-balance argument requires a time-dependent angular acceleration law.

Questions concerning transient spin-up, torque transmission, changing angular velocity, and the preparation or stability of the final state are separate dynamical problems. They are not used as premises for the stationary solution presented in this paper.

C Phenomenological Orbital Transfer Test with S2

C.1 Status of the test

The derivation in the main text concerns a closed material ring whose circumference is continuously occupied by matter. An isolated star on an orbit is not such a ring. The present appendix therefore does not assert that the stationary material-ring derivation automatically applies to an orbital tracer.

Instead, this appendix introduces a deliberately separate transfer hypothesis as a falsifiable observational template. No conclusion in the main stationary argument depends on the success of this transfer. Its purpose is to determine the magnitude and time dependence of the residual that would be produced if the same radial factor were associated phenomenologically with instantaneous orbital tangential speed.

C.2 Dimensionless transfer template

Let $\boldsymbol{r}_{\rm std}(t)$ be the position predicted by a baseline orbital model, let

$$r_{\rm std}(t) = |\boldsymbol{r}_{\rm std}(t)|,$$

and let $v_t(t)$ be the tangential component of its orbital velocity relative to the central source. Introduce a dimensionless transfer coefficient η and define

$$\boxed{\boldsymbol{r}_\eta(t) = \frac{\boldsymbol{r}_{\rm std}(t)}{\sqrt{1 + \eta\, v_t(t)^2/c^2}}.} \tag{19}$$

The cases have the following operational meanings:

- $\eta = 0$ reproduces the baseline orbit;
- $\eta = 1$ is the direct numerical transfer of the stationary radial factor;

- intermediate values represent a weaker effect;
- a fitted value consistent with zero would place an observational upper limit on this transfer.

Equation (19) is not presented as a derived orbital equation of motion. In particular, it does not by itself specify a modified force law, energy conservation law, or phase-field dynamics. It is a residual template to be tested against data.

C.3 First-stage implementation for S2

The numerical implementation uses the published S2 osculating orbital parameters from the GRAVITY analysis of the 2018 pericentre passage and the subsequent Schwarzschild-precession measurement [12, 13]. The values used in the reproducibility script are

$$M_\bullet = 4.261 \times 10^6 M_\odot, \qquad R_0 = 8246.7\,\mathrm{pc},$$

$$a = 125.058\,\mathrm{mas}, \qquad e = 0.884649, \qquad P = 16.0455\,\mathrm{yr},$$

with inclination 134.567°, argument of pericentre 66.263°, longitude of the ascending node 228.171°, and pericentre epoch 2018.37900.

Kepler's equation was solved over one orbital period, the orbital plane was rotated into the sky plane, and the transfer factor was evaluated using the tangential component of the baseline velocity. This is a first-stage osculating-orbit calculation. It is not a replacement for the full orbital model used by GRAVITY, which includes reference-frame parameters, finite light-travel time, special-relativistic and gravitational redshift terms, and relativistic precession [13].

C.4 Numerical signal for unit transfer amplitude

For $\eta = 1$, the simulation gives the following values near the 2018 pericentre:

Baseline pericentre radius	118.963310 AU
Tangential speed	$7738.277\,\mathrm{km\,s^{-1}}$
Inward radial residual	0.03961077 AU
Equivalent physical displacement	5.9257×10^6 km
Projected residual at pericentre	$3.6412\,\mu$as
Maximum projected residual	$4.0868\,\mu$as
Epoch of maximum projected residual	16.1 days before pericentre
Maximum line-of-sight velocity residual	$1.4419\,\mathrm{km\,s^{-1}}$

The scale of the baseline values is consistent with the reported passage of S2 at approximately 120 AU and $7700\,\mathrm{km\,s^{-1}}$ [12, 13].

C.5 Weak-effect scaling at pericentre

For $v_t/c \ll 1$, the radial residual generated by the template is

$$\Delta r \simeq -\frac{\eta}{2} r \frac{v_t^2}{c^2}.$$

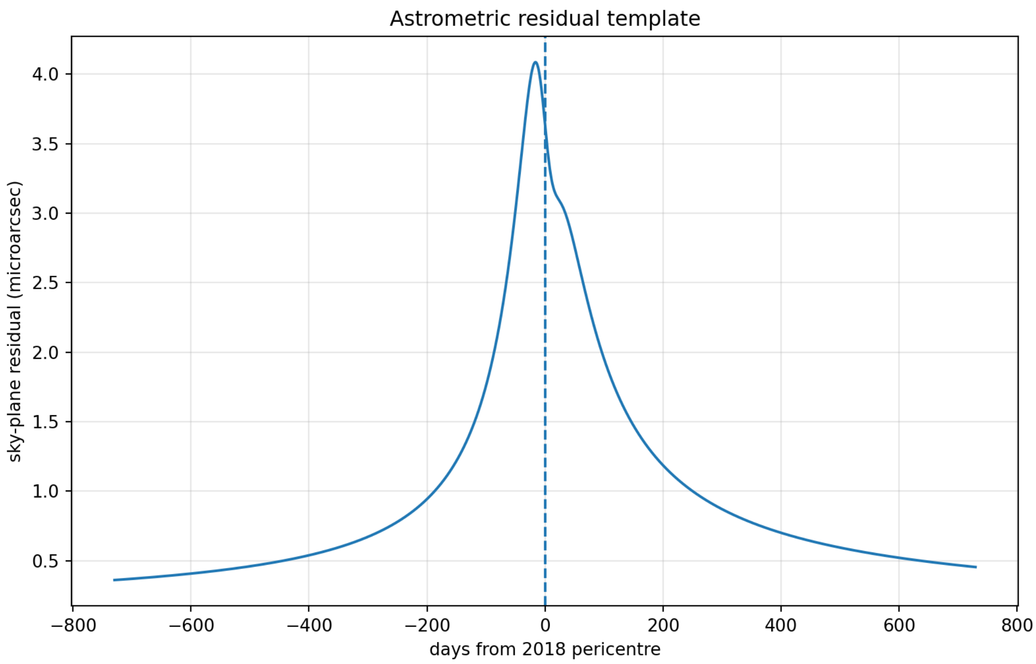

Figure 1: Sky-plane residual generated by the phenomenological transfer template with $\eta = 1$. The calculation uses a fixed osculating baseline and does not refit the orbital or reference-frame parameters.

For a Keplerian pericentre,

$$v_p^2 = \frac{GM_\bullet(1+e)}{r_p},$$

so the leading pericentre shift becomes

$$\boxed{|\Delta r_p| \simeq \frac{\eta}{2}\,\frac{GM_\bullet(1+e)}{c^2}.} \tag{20}$$

Within this template, decreasing the pericentre distance increases the speed but decreases the radius on which the fractional correction acts. The leading absolute shift is consequently nearly independent of pericentre distance for a fixed central mass and eccentricity. A closer star may still be observationally superior because of a shorter period, repeated pericentre passages, greater brightness, or improved astrometric precision.

C.6 Current-data scale and detectability

The 2020 GRAVITY analysis reports 54 interferometric measurements of the S2–Sgr A* separation between 2016.7 and 2019.7, with an rms uncertainty of approximately 65 μas, including 25 measurements in 2018. It also reports 92 spectroscopic measurements with an uncertainty of approximately 12 km s^{-1} [13].

A synthetic fixed-orbit forecast using a comparable number of epochs gives only an indicative sensitivity. With all standard orbital parameters held fixed, the combined template signal has approximate signal-to-noise ratios of 0.27, 1.28, 2.54, and 4.22 for per-coordinate astrometric uncertainties of 65, 10, 5, and 3 μas, respectively, while retaining a 12 km s^{-1} spectroscopic uncertainty. These numbers must not be interpreted as a fit to the published measurements.

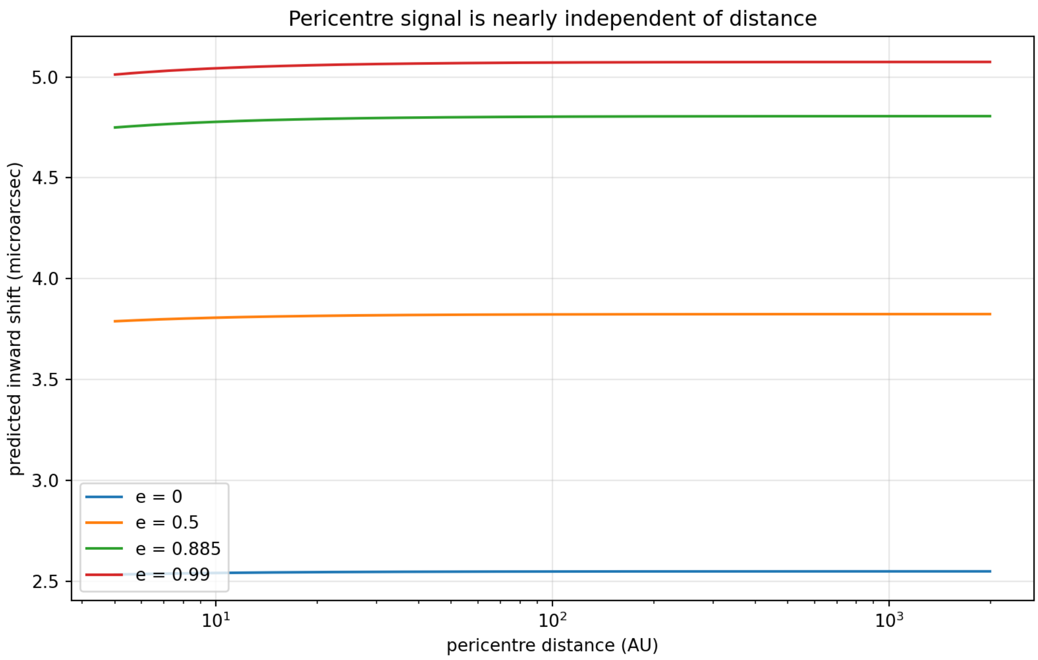

Figure 2: Pericentre residual predicted by the unit-amplitude transfer template for test Kepler orbits around the same central mass. The near-constancy at fixed eccentricity follows from Eq. (20).

A real inference will generally be less sensitive because η must be fitted simultaneously with the central mass, Galactic-centre distance, orbital elements, pericentre epoch, reference-frame offsets and drifts, Rømer delay, redshift terms, relativistic precession, and correlated systematic errors. Some part of the template may be absorbed by changes in semimajor axis, eccentricity, or pericentre time.

C.7 Required observational test

The appropriate analysis is a joint comparison of two models fitted to the same astrometric and spectroscopic measurements:

1. the baseline relativistic orbital model with $\eta = 0$;
2. the same model with η included as a fitted parameter.

A credible nonzero result would require all of the following:

- improvement in both sky-position and line-of-sight-velocity residuals;
- stability under changes in nuisance-parameter priors and data weighting;
- persistence when reference-frame and confusion systematics are varied;
- consistency of the fitted coefficient across more than one short-period star, when comparable data become available.

A result consistent with $\eta = 0$ would not affect the internal stationary ring derivation. It would show that the proposed transfer from a continuously occupied material ring to an isolated orbital tracer is absent or smaller than the observational limit. A result near $\eta = 1$ would motivate a separate theoretical derivation of the orbital transfer; it would not, by itself, supply that derivation.

C.8 Reproducibility and present limitation

The supplementary Python program `s2_radial_accommodation_template.py` generates the time series, key-epoch table, detectability estimate, and figures used in this appendix. The supplied calculation uses published best-fit orbital parameters and synthetic sampling only. No raw GRAVITY, NACO, SINFONI, or Keck measurement table has yet been fitted. The next quantitative step is therefore a full joint likelihood or Bayesian analysis using the actual observational data.

References

[1] P. Ehrenfest, original work on uniformly rotating rigid bodies and Born rigidity (1909).

[2] G. Herglotz, early work on relativistic rigid motion.

[3] F. Noether, early work on relativistic rigid motion.

[4] Z. Hu, "A Modern View of the Classical Herglotz–Noether Theorem."

[5] G. Weinstein, "Einstein's Uniformly Rotating Disk and the Hole Argument."

[6] J. Kumar, "Ehrenfest Paradox: A Careful Examination."

[7] R. Beig and B. G. Schmidt, "Relativistic Elasticity."

[8] P. Mourão, J. Natário, and R. Vicente, "Relativistic Elastic Membranes: Rotating Disks and Dyson Spheres."

[9] Ø. Grøn, "Relativistic Description of a Rotating Disk," *American Journal of Physics* **43**, 869 (1975).

[10] W. Rindler, *Relativity: Special, General, and Cosmological*, 2nd ed., Oxford University Press (2006).

[11] T. Weber, "A Note on the Ehrenfest Paradox," *Foundations of Physics Letters* **12**, 593 (1999).

[12] GRAVITY Collaboration, R. Abuter et al., "Detection of the gravitational redshift in the orbit of the star S2 near the Galactic centre massive black hole," *Astronomy & Astrophysics* **615**, L15 (2018).

[13] GRAVITY Collaboration, R. Abuter et al., "Detection of the Schwarzschild precession in the orbit of the star S2 near the Galactic centre massive black hole," *Astronomy & Astrophysics* **636**, L5 (2020).